A new approach for the incorporation of eigenstresses in arterial wall simulations

Jörg Schröder Sarah Brinkhues
j.schroeder@uni-due.de, sarah.brinkhues@uni-due.de

Abstract

In this report a novel approach for the modelling of residual stresses in human arteries is proposed. The starting point in a variety of contributions is the opening angle of the section of an artery as a consequence of a longitudinal cut. In contrast to this, we focus directly on the gradients of the fiber stresses in radial direction. As an underlying optimization criterion we assume that these gradients have to be smoothed between its inner and outer margins of the individual layers in an appropriate way. In order to do this we define "small" radial sections for the media and adventitia, where this condition has to be enforced independently. The efficiency of the proposed model is demonstrated by means of a patient-specific cross section of a diseased artery in a two-dimensional simulation.

1 Introduction

The assumption that a cylindrical arterial segment, which is not loaded with any external force, is stress free was disproved experimentally by Vaishnav & Vossoughi [46]. They sliced circular rings of bovine and porcine abdominal aortas radially. After the radial sectioning the rings opened up into a horseshoe leading to the conclusion that the aorta is residually stressed in circumferential direction when it is intact but free from external forces. However, Bergel [7] seems to be the first who observed this phenomenon. In Chuong & Fung [12] it was stated that residual stresses reduce the magnitude of the stresses and the stress gradient of a pressurized artery significantly, see also Fung [14]. Takamizawa & Hayashi [45] suggested that the residual stresses cause an almost uniform circumferential strain distribution under physiological pressure; this is called the uniform-strain hypothesis. In Nollert *et al.* [30] it is stated that a reduction of the stress gradient at the inner side of the arterial wall may reduce the risk of atherogenesis. Further experimental observations on rat aortas showed that the level of the segmental opening differs depending on the position of the segment in the aortic tree, see Liu & Fung [27]. Thus, the opening angle θ gradually varies from the ascending aorta to the lumbar region: it starts by 160°, follows a curve to 60°, tends toward zero before becoming slightly negative and increases again over 60°. Liu & Fung [28] banded abdominal rat aortas near the celiac trunk in order to establish hypertension. Then they discussed the change of the opening angle as a result of hypertension and hypertrophy and found out that a change in blood pressure changes the residual strains and therefore the opening angle significantly. They stated that the residual-strain change is stress-modulated. A study on the circumferential residual stresses in the left ventricle and the trachea is given in Omens & Fung [33] and Han & Fung [19], respectively. The zero-stress state of small blood vessels, which consists of 79–57% smooth muscles, was investigated by Fung & Liu [15]. Additionally, the effect of several drugs on

the microvessels were presented. Experiments on bovine aortas done by Vossoughi *et al.* [48] showed that even the cutted configuration is not fully stress-free. Additional circumferential cuts caused different opening angles for the individual arterial layers. Thus, the magnitude of opening of the inner layers increases while those of the outer layers reduces indicating that stresses still remain after the radial cut. Experiments on human aortas in Schulze-Bauer *et al.* [41] revealed also that residual stresses are not vanishing by a single cut, see also the study of Matsumoto *et al.* [29] on porcine thoracic aortas. Greenwald *et al.* [18] investigated aortas from rats and provided similar results concerning the different opening angles of the individual layers after mechanical removal of the other layers. Additionally, they showed that elastase treated (elimination of elastin) specimens offer smaller opening angles while collagenase treated (elimination of collagen) and frozen (destruction of smooth muscle cells) specimens behave like the untreated control specimens. First studies on human thoracic and abdominal aortas were done by Saini *et al.* [38]. Here, the influence of age, sex, the position along the artery, and atherosclerosis on the opening of sliced arterial rings was discussed. It was stated that the value of the opening angle increases with increasing distance from the heart (female: 150°–200°, male: 200°–250°). They also observed larger opening angles in aged and atherosclerotic diseased vessels, and in those obtained from male samples. Three-dimensional residual deformations of intact human abdominal aortas were shown in Holzapfel *et al.* [25]. In this study arterial rings were cut open and then separated into three layers. Furthermore, residual deformations on axial strips were investigated. It was stated that, due to the occurrence of the residual deformations in three dimensions, they cannot be described by a single parameter. A review of experimental methods for residual-strain measurement was given by Rachev & Greenwald [36]. Chuong & Fung [12] were probably the first to use a constitutive model to compute residual stresses. They discussed a procedure for the description of the geometry of an open artery, whose closed counterpart was regarded as thick-walled cylindrical tube with constant thickness. This method is known as *opening-angle method*. Therewith they computed the two-dimensional residual stresses in the unloaded closed artery and showed that the residual stresses enforce compression on the inner side of the vessel wall and tension on the outer side of the vessel wall. Many works are based on the opening-angle method to achieve an analytical solution for the residual strains of initially open ideal tubes, which were closed by an initial bending. Rachev [35] derived a mathematical model for the stress-dependent remodeling of a two-layer arterial tube. The assumption that the stress and strain values are equal under hypertensive and normotensive conditions was taken into account by means of remodeling of the zero-stress configuration by thickening of the layers. They also observed remaining residual stresses in the opened-up configuration of a hypertensive artery. Using a one-layer model Chaudhry *et al.* [10] showed that circumferential stresses and gradients are reduced significantly at the inner wall. The opening-angle method was also used by Holzapfel for an analytical solution of the initial deformation tensor for multilayered arterial tubes. In Holzapfel *et al.* [23] the opening-angle method was applied to a two-layered tube and different material models were investigated. Another key objective was to analyze the effect of the residual stresses onto the overall stress distribution in the physiological regime. The high-pressure response is analyzed in Holzapfel & Gasser [21]. Peña *et al.* [34] applied the opening-angle method to more realistic arterial geometries and conducted corresponding finite-element simulations. To account for residual stresses, Alastrué *et al.* [1] used a special form of the multiplicative decomposition of the deformation gradient, in which one part corresponds to the opening angle experiment. This approach was also investigated by Alastrué *et al.* [2], where growth was included, and implemented in a micro-sphere model in Alastrué *et al.* [3]. A combination of the

opening-angle method and a constrained mixture model of vascular growth and remodeling was suggested in Cardamone *et al.* [9]. Here, the mixture components are the individual constituents of the artery, i.e. elastin, collagen and smooth muscle. One aim of the authors was find the origin of residual stress. For the modeling of growth and remodeling in the framework of constrained mixture models see also Alford *et al.* [4] and Valentin [47]. Holzapfel & Ogden [22] accounted for the different behavior of the three main arterial layers and used different opening angles for the individual layers. Additionally, they extended the opening-angle method by accounting for bending and stretching in both circumferential and axial directions in order to reflect the three-dimensional residual stretch and stress state. A further extension of the model was done by Bustamante & Holzapfel [8], which accounted for opening angles depending on axial and radial position, i.e. different opening angles along the tube. Furthermore, a different set of opening angles for intima, media and adventitia were considered. Ståhlhand *et al.* [44] used experimental data in order to derive a residual-strain state. In order to do so, a minimization problem was derived for an approximate identification of material parameters including the residual strains. The parameters for the residual strains were presumed in the sense of the opening-angle method. This parameter identification algorithm is used in Olsson *et al.* [32] to determine an initial local deformation tensor, which is able to describe the residual strain, see also Klarbring *et al.* [26]. An extension of the model was given by Olsson [31], which introduced the evolution of growth. In the recent paper of Chen & Eberth [11] a uniform circumferential stress was obtained by introducing a special class of constitutive functions without considering a residually stressed state. This idea could be attractive for the design of engineered blood vessels. In contrast to the above mentioned methods Balzani *et al.* [5, 6] used a numerical method in order to establish a residual-strain state. Here, an initially open artery was numerically closed within a displacement-driven procedure. This model is appropriate, but nevertheless numerically extensive. In this work a novel model for the incorporation of residual stresses is proposed. An advantage of this model is that it is suitable for the incorporation of residual stresses in patient-specific arterial models.

2 Continuum mechanical framework

Let $\mathcal{B} \subset \mathbb{R}^3$ be the body of interest in the reference placement, parametrized in $\boldsymbol{X}$, and let $\mathcal{S}$ be the body in the current placement, parametrized in $\boldsymbol{x}$. The boundary $\partial\mathcal{B}$ of $\mathcal{B}$ is decomposed in $\partial\mathcal{B}_u$ and $\partial\mathcal{B}_t$ with $\partial\mathcal{B}_u \cup \partial\mathcal{B}_t = \partial\mathcal{B}$ and $\partial\mathcal{B}_u \cap \partial\mathcal{B}_t = \varnothing$. The nonlinear deformation map is given by $\boldsymbol{x} = \boldsymbol{\varphi}(\boldsymbol{X})$. As a basic kinematical quantity we define the deformation gradient and the right Cauchy-Green tensor

$$\boldsymbol{F} = \mathrm{Grad}\,\boldsymbol{\varphi}(\boldsymbol{X}) \quad \text{and} \quad \boldsymbol{C} = \boldsymbol{F}^T\boldsymbol{F}\ . \tag{1}$$

In order to fulfill the principle of material frame indifference a priori we formulate the free energy function ψ in terms of the right Cauchy-Green tensor, $\psi(\boldsymbol{C}) = W(\boldsymbol{F})$. Soft biological tissues as they occur in arterial walls have an anisotropic material behavior. To take into account for this aspect we formulate the anisotropic behavior by an isotropic tensor function of the form

$$\psi = \psi(I_1, I_2, I_3, J_4, J_5)\ , \tag{2}$$

with the principle invariants

$$I_1 = \mathrm{tr}\boldsymbol{C}\ , \quad I_2 = \mathrm{tr}[\mathrm{cof}\boldsymbol{C}] \quad \text{and} \quad I_3 = \mathrm{det}\boldsymbol{C}\ , \tag{3}$$

where $\mathrm{cof}\boldsymbol{C} = \det(\boldsymbol{C})\boldsymbol{C}^{-T}$, and the mixed invariants

$$J_4^{(a)} = \mathrm{tr}[\boldsymbol{C}\boldsymbol{M}^{(a)}] \quad \text{and} \quad J_5^{(a)} = \mathrm{tr}[\boldsymbol{C}^2\boldsymbol{M}^{(a)}] \,. \tag{4}$$

The structural tensors occurring in eq. (4) are defined by $\boldsymbol{M}^{(a)} = \boldsymbol{A}^{(a)} \otimes \boldsymbol{A}^{(a)}$ for $a = 1, 2$, where the unit vectors $\boldsymbol{A}^{(a)}$ describe the orientations of the collagen fiber bundles, which are mainly responsible for the anisotropic behavior of the arterial wall. For the modelling of the mechanical behavior of the media and adventitia we choose the energy function

$$\psi(I_1, I_2, I_3, J_4, J_5) = \psi^{iso}(I_1, I_2, I_3) + \sum_{a=1}^{2} \psi^{ti}_{(a)}(I_1, I_2, I_3, J_4, J_5) \tag{5}$$

consisting of an isotropic part ψ^{iso} for the matrix-material and two superimposed transversely isotropic energies $\psi^{ti}_{(a)}$ for the fiber contributions. For the isotropic part of the energy we choose a compressible Mooney-Rivlin model

$$\psi^{iso} = c_1 I_1 + c_2 I_2 + c_3 I_3 - \delta \, \ln\sqrt{I_3} \,, \tag{6}$$

which is also used for the approximation of the plaque behavior. In order to achieve a stress-free reference configuration associated to the isotropic contribution we set $\delta = 2c_1 + 4c_2 + 2c_3$. The anisotropic energy introduced in Holzapfel *et al.* [23] is given by

$$\psi^{ti}_{(a)} = \frac{k_1}{2k_2} \left\{ \exp\left[k_2 \langle J_4^{(a)} - 1 \rangle^2 \right] - 1 \right\} \,, \tag{7}$$

with the material parameters k_1 and k_2. In biomechanical applications we often assume that the material behaves quasi-incompressible. This condition is enforced by an augmented Lagrangian solution strategy, in this context we refer to Glowinski & Le Tallec [16, 17] and Simo & Taylor [42].

3 Computation of residual stresses

Generally, in case of kinematically constrained materials, such as quasi-incompressible soft biological tissues, the true stresses $\boldsymbol{\sigma}$ are decomposed into deviatoric and hydrostatic parts. Furthermore, fiber-reinforced tissues like arterial walls exhibit a distinct behavior in the direction of the fibers. Therefore, the Cauchy stresses are additively decomposed into deviatoric ground stresses $\boldsymbol{\sigma}^*$, which depend on the deformation, and reaction stresses $\boldsymbol{\sigma}^r$

$$\boldsymbol{\sigma} = \boldsymbol{\sigma}^* + \boldsymbol{\sigma}^r \,. \tag{8}$$

The second part of the stresses, $\boldsymbol{\sigma}^r$, is a reaction to the constraints and cannot be computed from constitutive equations. For the definition of suitable invariants we assume (in addition to the incompressibility of the material) the (fictive) inextensibility of the fibers. Since the material is assumed to be incompressible and inextensible in the current fiber directions $\boldsymbol{a}_{(1)}$ and $\boldsymbol{a}_{(2)}$, the reaction is composed of a hydrostatic pressure p and tensions $T_{(1)}$ and $T_{(2)}$ in the direction of inextensibility $\boldsymbol{a}_{(1)}$ and $\boldsymbol{a}_{(2)}$, respectively. Thus, the reaction stress tensor $\boldsymbol{\sigma}^r$ results from the equilibrium conditions in consideration of the side conditions of the boundary value problem and arises as

$$\boldsymbol{\sigma}^r = -p\,\mathbf{1} + T_{(1)}\,\tilde{\boldsymbol{m}}_{(1)} + T_{(2)}\,\tilde{\boldsymbol{m}}_{(2)} \,. \tag{9}$$

Here, $\tilde{\boldsymbol{m}}_{(a)} = \tilde{\boldsymbol{a}}_{(a)} \otimes \tilde{\boldsymbol{a}}_{(a)}$ are the structural tensors associated to the preferred directions $\tilde{\boldsymbol{a}}_{(a)}$ in the current placement. Following eq. (9) the expressions $\mathrm{tr}\,\boldsymbol{\sigma}^*$, $\boldsymbol{\sigma}^* : \tilde{\boldsymbol{m}}_{(1)}$ and

$\boldsymbol{\sigma}^* : \tilde{\boldsymbol{m}}_{(2)}$ are absorbed into the functions $p, T_{(1)}$ and $T_{(2)}$ leading to the side conditions on the ground stresses

$$\mathrm{tr}\boldsymbol{\sigma}^* = 0 \,, \quad \boldsymbol{\sigma}^* : \tilde{\boldsymbol{m}}_{(1)} = 0 \quad \text{and} \quad \boldsymbol{\sigma}^* : \tilde{\boldsymbol{m}}_{(2)} = 0 \,. \tag{10}$$

The general idea of this approach is based on Spencer [43] and Rogers [37], see also Schröder [39]. It should be noticed, that the assumption of inextensible fibers is intended for the motivation of suitable invariants only. This assumption is not taken into account in the constitutive modeling of the arterial behavior. In consideration of eq. (9) and eq. (10) the projection of the stresses onto the current preferred directions and the evaluation of the volumetric part of the stresses lead to the hydrostatic pressure p and the fiber stresses $T_{(1)}$ and $T_{(2)}$.

The incorporation of residual stresses is based on a decomposition of the domain, which is carried out in two consecutive steps. First, the arterial cross-section, which consists of $\mathrm{n_{MAT}}$ layers or materials, respectively, is initially decomposed into $\mathrm{n_{SG}}$ segments. Then, each segment is further subdivided into $\mathrm{n_{MAT}}$ sectors, depending on the number of materials the segments consists of. Considering a two-dimensional arterial cross-section, the number of sectors can be specified as

$$\mathrm{n_{SC}} = \mathrm{n_{SG}} \cdot \mathrm{n_{MAT}} \,. \tag{11}$$

In Figure 1 the decomposition of a two-dimensional arterial cross-section consisting of two layers ($\mathrm{n_{MAT}} = 2$) is depicted schematically. In this example the amount of segments is $\mathrm{n_{SG}} = 16$, thus the cross-section decomposed into $\mathrm{n_{SC}} = 32$ sectors.

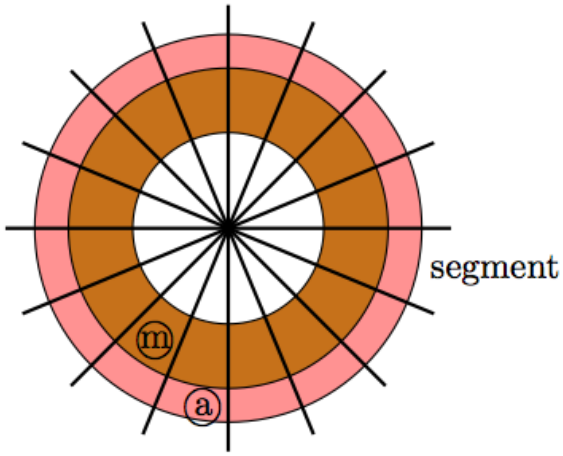

Figure 1: Schematical illustration of the decomposition of an arterial cross-section, which consists of two materials (media ⓜ and adventitia ⓐ, i.e. $\mathrm{n_{MAT}} = 2$).

When the artery is loaded with a physiological internal pressure, the local volume average values of the fiber stresses are computed for each sector with the subvolumes V_i, i.e.

$$\overline{T}^i_{(1)} = \frac{1}{V_i} \int_{\mathcal{B}_i} T_{(1)}(\boldsymbol{x}) \, \mathrm{d}v \quad \text{and} \quad \overline{T}^i_{(2)} = \frac{1}{V_i} \int_{\mathcal{B}_i} T_{(2)}(\boldsymbol{x}) \, \mathrm{d}v \,, \tag{12}$$

with $i = 1, \ldots, \mathrm{n_{SC}}$ and $\boldsymbol{x} \in \mathcal{B}_i$. The difference between this mean value and the fiber stresses yields the stresses

$$\Delta T_{(1)} = T_{(1)} - \overline{T}^i_{(1)} \quad \text{and} \quad \Delta T_{(2)} = T_{(2)} - \overline{T}^i_{(2)} \quad \text{in } \mathcal{B}_i \,. \tag{13}$$

These stresses in turn are used for an estimation of the residual stresses

$$\boldsymbol{\sigma}^{\mathrm{res}} = -\Delta p\, \mathbf{1} + \Delta T_{(1)}\, \tilde{\boldsymbol{m}}_{(1)} + \Delta T_{(2)}\, \tilde{\boldsymbol{m}}_{(2)} \,. \tag{14}$$

Since the residual stresses should not cause changes in volume, Δp can be computed from the condition $\mathrm{tr}\, \boldsymbol{\sigma}^{\mathrm{res}} = 0$ and yields $\Delta p = \frac{1}{3}\left(\Delta T_{(1)} + \Delta T_{(2)}\right)$. The estimation of the residual stresses is accomplished within an iterative process. Here, the so-called smoothing-loops (SL) are applied with a certain amount of the computed residual stresses in eq. (14) in a stepwise manner. After that the residual stresses are stored and considered in the following simulations in form of the second Piola-Kirchhoff tensor

$$\boldsymbol{S}^{\mathrm{res}} = J\boldsymbol{F}^{-1}\, \boldsymbol{\sigma}^{\mathrm{res}}\, \boldsymbol{F}^{-T} \,. \tag{15}$$

4 Numerical simulation of a realistic artery

In this section the simulation of a two-dimensional patient-specific arterial cross-section, see Figure 2, in consideration of residual stresses is discussed. It consists of the two arterial layers adventitita and media and a large plaque inclusion.

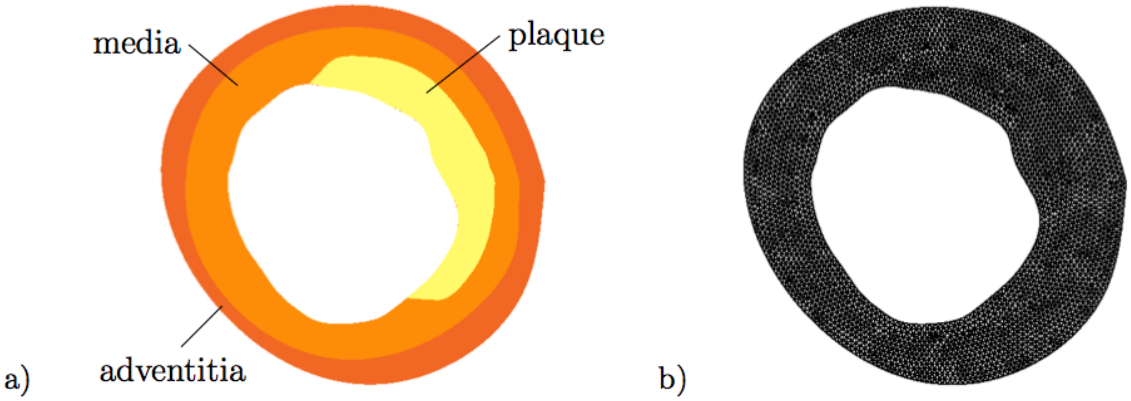

Figure 2: a) Two-dimensional numerical model of an arterial wall and b) discretization of the cross-section with 6 015 quadratic triangular finite elements.

The material parameters used in this simulation are listed in Table 2.

	c_1 [kPa]	c_2 [kPa]	c_3 [kPa]	k_1 [kPa]	k_2 [-]	β_f [°]
media	14.638	0.149	60.810	6.851	754.014	43.468
adventitia	2.326	6.169	60.642	$3.131 \cdot 10^{-8}$	147.174	52.285
plaque	60.0	15.0	800.0	–	–	–

Table 2: Material parameter for media, adventitia and plaque.

For the incorporation of residual stresses the cross-section is decomposed into $\mathrm{n_{SC}} = 36 \cdot 2 = 72$ sectors, even though there exist three materials (adventitia, media, and plaque) $\mathrm{n_{MAT}} = 2$. This is due to the reasonable assumption that the plaque exhibits no fibers ($T_{(1)} = T_{(2)} = 0$) and thus no residual stresses. At an internal pressure of $p_i = 16.0$ kPa a number of 13 smoothing-loops are applied with 10% of magnitude. The σ_{22} stresses before and after the application of the smoothing-loops arise as depicted in Figure 3.

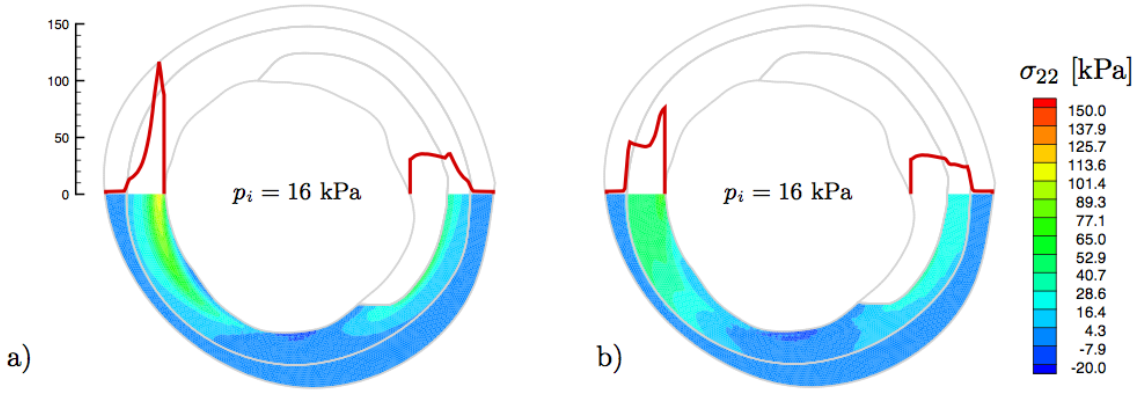

Figure 3: σ_{22}-stress distribution a) without and b) with residual stresses.

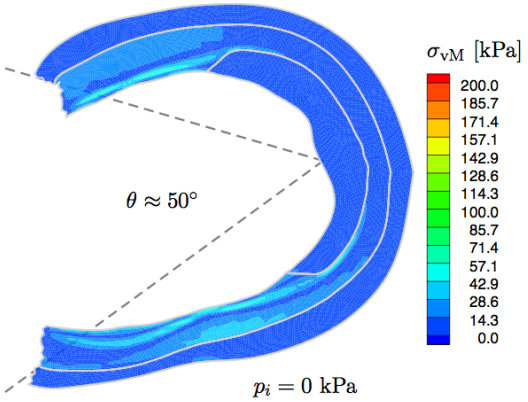

Figure 4: Distribution of the von Mises stress σ_{vM} [kPa] in an opened artery, where the opening angle arises as $\theta \approx 50°$. The opening is only due to residual stresses as the internal pressure is zero.

Throughout the whole procedure the adventitia is almost stress free. However, in the media the smoothing of the strong gradient as a result of the application of the residual stresses is clearly visible.

Next, we analyze the behavior of the unloaded artery with residual stresses after a radial cut. In order to do so, a sliced, but geometrically closed cross-section is taken into account. The residual-stress distribution, which has been computed in the previous numerical simulation, is applied on the cross-section. In Figure 4 the result of the simulation is shown. The artery opens due to the residual stresses and an opening angle of $\theta \approx 50°$ arises. The von Mises stresses, defined by $\sigma_{\mathrm{vM}} = \sqrt{3/2}\ \|\operatorname{dev}\boldsymbol{\sigma}\|$ with $\operatorname{dev}\boldsymbol{\sigma} = \boldsymbol{\sigma} - \frac{1}{3}\operatorname{tr}\boldsymbol{\sigma}\,\mathbf{1}$, are close to zero in the opened state. However, the stresses are not exactly equal to zero, which is in agreement with the experimental findings of Vossoughi *et al.* [48].

5 Summary

The existence of residual stress reveals, when an arterial ring springs open after a cut in the radial direction. This happens due to the relieving of the circumferential residual stresses, which are compressive on the inner part of the ring and tensile on the outer part. In the present work, a novel approach was presented in order to account for such residual stresses. For this, we focused directly on the gradients of the fiber stresses in radial direction. As

an underlying optimization criterion we assumed that these gradients have to be smoothed between its inner and outer margins of the individual layers in an appropriate way. In order to do this we defined radial sections for the media and adventitia, where this condition has to be enforced independently. The efficiency of the proposed model is demonstrated by means of an academic tube model and a patient-specific cross section of a diseased artery. In detail, the numerical results of the tube model shows the smoothing of the gradients and the opening of the tube after radial cut due to the residual stresses. Furthermore, the numerical simulation shows the applicability of the model onto a real arterial geometry.

Acknowledgements

We gratefully acknowledge support by the Deutsche Forschungsgemeinschaft (DFG) through the research grants SCHR 570/16-1.

References

[1] V. Alastrué, E. Peña, M. Ángel, M.A. Martínez, and M. Doblaré. Assessing the use of the "opening angle method" to enforce residual stresses in patient-specific arteries. *Annals of Biomedical Engineering*, 35:1821–1837, 2007.

[2] V. Alastrué, M.A. Martínez, and M. Doblaré. Modelling adaptive volumetric finite growth in patient-specific residually stressed arteries. *Journal of Biomechanics*, 41: 1773–1781, 2008.

[3] V. Alastrué, M.A. Martínez, M. Doblaré, and A. Menzel. Anisotropic micro-sphere-based finite elasticity applied to blood vessel modelling. *Journal of the Mechanics and Physics of Solids*, 57:178–203, 2009.

[4] P.W. Alford, J.D. Humphrey, and L.A. Taber. Growth and remodeling in a thick-walled artery model: effects of spatial variations in wall constituents. *Biomechanics and Modeling in Mechanobiology*, 7(4):245–262, 2008.

[5] D. Balzani, J. Schröder, and D. Gross. Simulation of discontinuous damage incorporating residual stresses in circumferentially overstretched atherosclerotic arteries. *Acta Biomaterialia*, 2:609–618, 2006.

[6] D. Balzani, J. Schröder, and D. Gross. Numerical simulation of residual stresses in arterial walls. *Computational Materials Science*, 39:117–123, 2007.

[7] D.H. Bergel. *The visco-elastic properties of the arterial wall.* PhD thesis, University of London, London, 1960.

[8] C. Bustamante and G.A. Holzapfel. Methods to compute 3D residual stress distributions in hyperelastic tubes with application to arterial walls. *International Journal of Engineering Science*, 48(11):1066–1082, 2010.

[9] L. Cardamone, A. Valentin, J.F. Eberth, and J.D. Humphrey. Origin of axial prestretch and residual stress in arteries. *Biomechanics and Modeling in Mechanobiology*, 8:431–446, 2009.

[10] H.R. Chaudhry, B. Bukiet, A. Davis, A.B. Ritter, and T. Findley. Residual stresses in oscillating thoracic arteries reduce circumferential stresses and stress gradients. *Journal of Biomechanics*, 30(1):57–62, 1997.

[11] Y.-C. Chen and J.F. Eberth. Constitutive function, residual stress, and state of uniform stress in arteries. *Journal of the Mechanics and Physics of Solids*, 60(6):1145–1157, 2012.

[12] C.J. Chuong and Y.C. Fung. On residual stress in arteries. *Journal of Biomechanical Engineering*, 108:189–191, 1986.

[13] P.G. Ciarlet. *Mathematical Elasticity, Volume 1: Three Dimensional Elasticity*. Elsevier Science Publishers B.V., North Holland, 1988.

[14] Y.C. Fung. What are the residual stresses doing in our blood vessels? *Annals of Biomedical Engineering*, 19(3):237–249, 1991.

[15] Y.C. Fung and S.Q. Liu. Strain distribution in small blood vessels with zero-stress state taken into consideration. *American Journal of Physiology – Heart and Circulatory Physiology*, 262:H544–H552, 1992.

[16] R. Glowinski and P. Le Tallec. Finite element analysis in nonlinear incompressible elasticity. In J.T. Oden and G.F. Carey, editors, *Finite elements, Vol V: Special Problems in Solid Mechanics*. Prentice-Hall, Englewood Cliffs, NH, 1984.

[17] R. Glowinski and P. Le Tallec. *Augmented Lagrangian methods for the solution of variational problems*. Springer, Berlin, 1988.

[18] S.E. Greenwald, J.E. Moore, A. Rachev, T.P.C. Kane, and J.-J. Meister. Experimental investigation of the distribution of residual strains in the artery wall. *Journal of Biomechanical Engineering*, 119:438–444, 1997.

[19] H.C. Han and Y.C. Fung. Residual strains in porcine and canine trachea. *Journal of Biomechanics*, 24:307–315, 1991.

[20] G.A. Holzapfel. Determination of material models for arterial wallls from uniaxial extension tests and histological structure. *Journal of Theoretical Biology*, 238:290–302, 2006.

[21] G.A. Holzapfel and T.C. Gasser. Computational stress-deformation analysis of arterial walls including high-pressure response. *International Journal of Cardiology*, 116:78–85, 2007.

[22] G.A. Holzapfel and R.W. Ogden. Modelling the layer-specific 3d residual stresses in arteries, with an application to the human aorta. *Journal of the Royal Society Interface*, 7:787–799, 2010.

[23] G.A. Holzapfel, T.C. Gasser, and R.W. Ogden. A new constitutive framework for arterial wall mechanics and a comparative study of material models. *Journal of Elasticity*, 61:1–48, 2000.

[24] G.A. Holzapfel, G. Sommer, and P. Regitnig. Anisotropic mechanical properties of tissue components in human atherosclerotic plaques. *Journal of Biomechanical Engineering*, 126:657–665, 2004.

[25] G.A. Holzapfel, G. Sommer, M. Auer, P. Regitnig, and R.W. Ogden. Layer-specific 3d residual deformations of human aortas with non-atherosclerotic intimal thickening. *Annals of Biomedical Engineering*, 35(4):530–545, 2007.

[26] A. Klarbring, T. Olsson, and J. Ståhlhand. Theory of residual stresses with application to an arterial geometry. *Archives of Mechanics*, 59(4-5):341–364, 2007.

[27] S.Q. Liu and Y.C. Fung. Zero-stress states of arteries. *Journal of Biomechanical Engineering*, 110:82–84, 1988.

[28] S.Q. Liu and Y.C. Fung. Relationship between hypertension, hypertrophy, and opening angle of zero-stress state of arteries following aortic constriction. *Journal of Biomechanical Engineering*, 111:325–335, 1989.

[29] T. Matsumoto, T. Goto, T. Furukawa, and M. Sato. Residual stress and strain in the lamellar unit of the porcine aorta: experiment and analysis. *Journal of Biomechanics*, 37(6):807–815, 2004.

[30] M.U. Nollert, N.J. Panaro, and L.V. McIntire. Regulation of genetic expression in shear stress–stimulated endothelial cellsa. *Annals of the New York Academy of Sciences*, 665(1):94–104, 1992.

[31] T. Olsson and A. Klarbring. Residual stresses in soft tissue as a consequence of growth and remodeling: application to an arterial geometry. *European Journal of Mechanics, A/Solids*, 27:959–974, 2008.

[32] T. Olsson, J. Ståhlhand, and A. Klarbring. Modeling initial strain distribution in soft tissues with application to arteries. *Biomechanics and Modeling in Mechanobiology*, 5: 28–38, 2006.

[33] J.H. Omens and Y.C. Fung. Residual strain in rat left ventricle. *Circulation Research*, 66(1):37–45, 1990.

[34] E. Peña, M.A. Martinez, B. Calvo, and M. Doblaré. On the numerical treatment of initial strains in biological soft tissues. *International Journal for Numerical Methods in Engineering*, 68:836–860, 2006.

[35] A. Rachev. Theoretical study of the effect of stress-dependent remodeling on arterial geometry under hypertensive conditions. *Journal of Biomechanics*, 30:819–827, 1997.

[36] A. Rachev and S.E. Greenwald. Residual strains in conduit arteries. *Journal of Biomechanics*, 36:661–670, 2003.

[37] T.G. Rogers. Yield criteria, flow rules, and hardening in anisotropic plasticity. In J.P. Boehler, editor, *Yielding, damage and failure of anisotropic solids*, pages 53–79, 1987.

[38] A. Saini, C. Berry, and S. Greenwald. Effect of age and sex on residual stress in the aorta. *Journal of Vascular Research*, 32:398–405, 1995.

[39] J. Schröder. *Theoretische und algorithmische Konzepte zur phänomenologischen Beschreibung anisotropen Materialverhaltens.* Phd-thesis, Universität Hannover, Institut für Mechanik (Bauwesen), Lehrstuhl I, Bericht Nr.: I-1, 1996.

[40] J. Schröder and P. Neff. Invariant formulation of hyperelastic transverse isotropy based on polyconvex free energy functions. *International Journal of Solids and Structures*, 40:401–445, 2003.

[41] C.A.J. Schulze-Bauer, M. Auer and G.A. Holzapfel. Layer-specific residual deformations of aged human aortas. *13th Conference of the European Society of Biomechanics*, 2002

[42] F.C. Simo and R.L. Taylor. Quasi-incompressible finite elasticity in principal stretches. continuum basis and numerical algorithms. *Computer Methods in Applied Mechanics and Engineering*, 85(3):273–310, 1991.

[43] A.J.M. Spencer. *Deformations of fibre-reinforced materials*. Oxford University Press, 1972.

[44] J. Ståhlhand, A. Klarbring, and M. Karlsson. Towards in vivo aorta material identification and stress estimation. *Biomechanics and Modeling in Mechanobiology*, 2: 169–186, 2004.

[45] K. Takamizawa and K. Hayashi. Strain energy density function and uniform strain hypothesis for arterial mechanics. *Journal of Biomechanics*, 20:7–17, 1987.

[46] R.N. Vaishnav and J. Vossoughi. Estimation of residual strains in aortic segments. In C.W. Hall, editor, *Biomedical Engineering II: Recent Developments*. Pergamon Press, New York, 1983.

[47] A. Valentin and J.D. Humphrey. Evaluation of fundamental hypotheses underlying constrained mixture models of arterial growth and remodelling. *Philosophical Transactions of the Royal Society A: Mathematical, Physical and Engineering Sciences*, 367 (1902):3585–3606, 2009.

[48] J. Vossoughi, Z. Hedjazi, and F.S. Borris. Intimal residual stress and strain in large arteries. In N.A. Langrana, M.H. Friedman, and E.S. Grood, editors, *Proceedings of the Summer Bioengineering Conference, New York*, pages 434–437. American Society of Mechanical Engineers, 1993.

Jörg Schröder, Universitätsstraße 15, 45117 Essen, Germany
Sarah Brinkhues, Universitätsstraße 15, 45117 Essen, Germany